

HawkEye: Advancing Robust Regression with Bounded, Smooth, and Insensitive Loss Function

Mushir Akhtar^a, M. Tanveer^{a,*}, Mohd. Arshad^a

^a*Department of Mathematics, Indian Institute of Technology
Indore, Simrol, Indore, 453552, Madhya Pradesh, India*

Abstract

Support vector regression (SVR) has garnered significant popularity over the past two decades owing to its wide range of applications across various fields. Despite its versatility, SVR encounters challenges when confronted with outliers and noise, primarily due to the use of the ϵ -insensitive loss function. To address this limitation, SVR with bounded loss functions has emerged as an appealing alternative, offering enhanced generalization performance and robustness. Notably, recent developments focus on designing bounded loss functions with smooth characteristics, facilitating the adoption of gradient-based optimization algorithms. However, it's crucial to highlight that these bounded and smooth loss functions do not possess an insensitive zone. In this paper, we address the aforementioned constraints by introducing a novel symmetric loss function named the HawkEye loss function. It is worth noting that the HawkEye loss function stands out as the first loss function in SVR literature to be bounded, smooth, and simultaneously possess an insensitive zone. Leveraging this breakthrough, we integrate the HawkEye loss function into the least squares framework of SVR and yield a new fast and robust model termed HE-LSSVR. The optimization problem inherent to HE-LSSVR is addressed by harnessing the adaptive moment estimation (Adam) algorithm, known for its adaptive learning rate and efficacy in handling large-scale problems. To our knowledge, this is the first time Adam has been employed to solve an SVR problem. To empirically validate the proposed HE-LSSVR model, we evaluate it on UCI, synthetic, and time series datasets. The experimental outcomes unequivocally reveal the superiority of the HE-LSSVR model both in terms of its remarkable generalization

*Corresponding author

performance and its efficiency in training time.

Keywords: Supervised learning, Support vector regression, Loss function, HawkEye loss function, Adam algorithm

1. Introduction

Machine learning, a subset of artificial intelligence, has witnessed remarkable advancements in recent years, revolutionizing various fields through its ability to extract meaningful patterns from complex data [1]. Within the realm of machine learning, supervised learning stands as a cornerstone, where algorithms learn from labeled datasets to make predictions or infer relationships between input and output variables [2]. Among the diverse applications of supervised learning, regression emerges as a fundamental subfield dedicated to modeling the intricate connections between input variables and continuous output values [3].

Support vector regression (SVR) [4] is a powerful and versatile machine learning technique designed for solving regression problems. It belongs to the family of support vector machines (SVMs) [5], which are renowned for their effectiveness in classification tasks. SVMs have applications in several areas, such as pattern classification [6], concept drift [7], credit risk evaluation [8], and many more. In a nutshell, SVMs are rooted in the framework of statistical learning theory, which equips them with the ability to generalize effectively to new and unseen data. However, SVR extends the capabilities of SVM to handle continuous output variables, making it a valuable tool for predictive modeling and function approximation. It has extensive applications across various domains, such as load forecasting [9], water temperature prediction [10], stock prediction [11], landslide prediction [12], petroleum resource prediction [13], health estimation of battery [14], estimation of bank profitability [15], flight control [16] and so forth.

Consider a regression training dataset $\{x_i, y_i\}_{i=1}^N$, where $x_i \in \mathbb{R}^m$ represents the input data point and $y_i \in \mathbb{R}$ corresponds to the target value associated with that input. The core idea of SVR is to estimate a linear function $f(x) = w^\top x + b$, where $b \in \mathbb{R}$ represents the bias and $w \in \mathbb{R}^m$ signifies the weight vector. These parameters are estimated through the process of training using available data. For a test data point \tilde{x} , the associated target value \tilde{y} is estimated as $w^\top \tilde{x} + b$. Analogously to SVM, we discuss two scenarios of SVR namely, hard SVR and soft SVR. For pedagogical reasons, we

begin by describing the case of hard SVR. In hard SVR, the goal is to find a linear regression function f that fits the training data while strictly enforcing that all data points are within a specified margin of error ε . Mathematically, the objective function for hard SVR is as follows:

$$\begin{aligned} \min_{w,b} \quad & \frac{1}{2} \|w\|^2 \\ \text{subject to} \quad & y_i - w^\top x_i - b \leq \varepsilon \\ & w^\top x_i + b - y_i \leq \varepsilon, \quad \forall i = 1, 2, \dots, N. \end{aligned} \tag{1}$$

The two constraints ensure that the predicted values for all data points must lie within a symmetric margin of tolerance ε around the true target values y_i . In other words, the error between the predicted values and the true target values is required to be no more than ε . The tacit assumption in (1) is that such a function f actually exists that approximates all pairs (x_i, y_i) with ε precision. However, this may not be the case in real-world applications. To address this challenge, a widely adopted strategy is to permit a certain degree of error in the model while simultaneously imposing penalties for these errors. This is accomplished by introducing a loss function into the objective function and called as soft SVR. The unconstrained optimization problem of soft SVR is as follows:

$$\min_{w,b} \quad \frac{1}{2} \|w\|^2 + C \sum_{i=1}^N \mathcal{L}(r_i), \tag{2}$$

where $r_i = y_i - f(x_i)$ represents the training error, $C > 0$ is a regularization parameter which controls the trade-off between model complexity and training errors, $\mathcal{L}(\cdot)$ is a loss function, and $\sum_{i=1}^N \mathcal{L}(r_i)$ expresses the empirical risk. In simpler terms, soft SVR prioritizes minimizing errors as long as they remain within the ε tolerance range, but it strongly penalizes any deviations exceeding this threshold.

In this paper, our primary focus revolves around enhancing the performance of SVR. In the realm of developing novel regression models, one critical aspect that garners significant attention is the design of appropriate loss functions. The traditional SVR models commonly employ convex and unbounded loss functions, such as the ε -insensitive loss function [4], the least squares loss function [17], and the Huber loss function [18], to penalize regression errors. These loss functions entail that as the error between predicted and true values

increases, the corresponding loss also increases without bounds. This characteristic can pose several challenges, particularly when dealing with noisy data, and may result in suboptimal model performance.

In real-world applications, it may be possible that data contains outliers. The term “outliers” pertains to instances that deviate significantly from the pattern established by the vast majority of the data [19]. Outliers are often difficult to recognize in high dimensional datasets by reason of the curse of dimensionality [20]. As a result, the learned model is unreliable. To mitigate the effect of outliers, many robust loss functions have been proposed. Over the last few decades, non-convex and bounded loss functions have gained prominence, primarily to enhance the robustness of models in the presence of noisy data. One well-known representative of such functions is the ramp loss function [21]. Its primary purpose is to restrict the maximum loss to a fixed value for data samples that exhibit significant deviations, which diminishes the effect of noise and outliers. Following the introduction of the ramp loss function, several variants have been developed, further extending the versatility of this approach. These variants include the non-convex least square loss function [22], ramp ε -insensitive loss function [23], generalized quantile loss function [24], quadratic non-convex ε -insensitive loss function [25] and canal loss function [26]. The key advantage of these loss functions lies in their bounded nature. They effectively constrain the loss to a predefined threshold, ensuring that the model remains robust even in the presence of noisy data. However, it is essential to recognize that the methodology of hard truncation employed in these loss functions, especially when addressing data points with substantial regression errors, can introduce non-smoothness into the loss function. Hence, the optimization problems associated with SVR models based on non-convex and non-smooth loss functions present algorithmic intricacies and demand considerable computational resources.

Based on insights gleaned from previous research efforts, this paper introduces the HawkEye loss, an innovative loss function meticulously designed to exhibit boundedness, smoothness, and the simultaneous presence of an insensitive zone. The key advantage of the smoothness property is that it allows the utilization of gradient-based optimization algorithms, ensuring well-defined gradients and enabling the application of fast and reliable optimization techniques. Subsequently, by incorporating the newly proposed HawkEye loss into the least squares version of SVR, we propose a new fast and robust model for handling large-scale problems called HE-LSSVR. The optimization problem associated with the HE-LSSVR is effectively addressed

through the utilization of the adaptive moment estimation (Adam) algorithm. The key contributions of this study can be succinctly summarized as follows:

- We introduce a novel development in the realm of supervised learning, the HawkEye loss function, meticulously crafted to exhibit boundedness, smoothness, and the simultaneous inclusion of an insensitive zone.
- We present a comparative analysis of the existing loss functions with the HawkEye loss function and showcase that it is the first loss function in SVR literature that is bounded, smooth, and simultaneously possesses an insensitive zone.
- We amalgamate the HawkEye loss function into the least squares framework of SVR and formulate a new fast and robust model coined as HE-LSSVR.
- We address the optimization problem of HE-LSSVR by harnessing the Adam algorithm, known for its adaptive learning rate and efficacy in handling large-scale problems. To our knowledge, this is the first time Adam has been employed to solve an SVR problem.
- We conduct numerical experiments on UCI, synthetic, and time series datasets and validate that the proposed HE-LSSVR model is superior compared to the baseline models both in terms of generalization performance and training time.

2. Related work

The design of loss functions is a fundamental component in the development of machine learning models [27]. It plays a pivotal role in assessing the dissimilarity between predicted values and their corresponding target values [28]. In this section, we provide a brief overview of commonly employed loss functions in regression. To facilitate comprehension, we present the mathematical formulation of these loss functions in Table 1, and offer graphical representations of some of them in Figure 1.

Table 1: Mathematical formulation of commonly used loss function in regression. Unless otherwise specified ε , θ , and t are non negative hyperparameters.

Category	Loss function	Formulation
Unbounded	Least square loss function	$\mathcal{L}(r) = r^2$
	Absolute loss function	$\mathcal{L}(r) = r $
	Huber loss function	$\mathcal{L}(r) = \begin{cases} \theta r - \frac{1}{2}\theta^2, & r \geq \theta \\ \frac{1}{2}r^2, & r < \theta \end{cases}$
	Insensitive loss function	$\mathcal{L}(r) = \max \{0, r - \varepsilon\}$
Bounded	Ramp insensitive loss function	$\mathcal{L}(r) = \begin{cases} 0, & r < \varepsilon \\ r - \varepsilon, & \varepsilon \leq r \leq \theta \\ \theta - \varepsilon, & r > \theta \end{cases}$
	Non-convex least square loss function	$\mathcal{L}(r) = \begin{cases} r^2, & r \leq \theta \\ \theta^2, & r > \theta \end{cases}$
	Ramp insensitive least square loss function	$\mathcal{L}(r) = \begin{cases} 0, & r < \varepsilon \\ (r - \varepsilon)^2, & \varepsilon \leq r \leq \theta \\ (\theta - \varepsilon)^2, & r > \theta \end{cases}$
	Quadratic non-convex insensitive loss function	$\mathcal{L}(r) = \begin{cases} 0, & r < \varepsilon \\ (r - \varepsilon)^2, & \varepsilon \leq r \leq t \\ (t - \varepsilon)^2 + \theta r - \theta t, & r > t \end{cases}$
	Canal loss	$\mathcal{L}(r) = \min \{\theta - \varepsilon, \max \{0, r - \varepsilon\}\}$
	Bounded least square loss function	$\mathcal{L}(r) = \frac{1}{t} \left(1 - \frac{1}{1+\theta r^2}\right)$

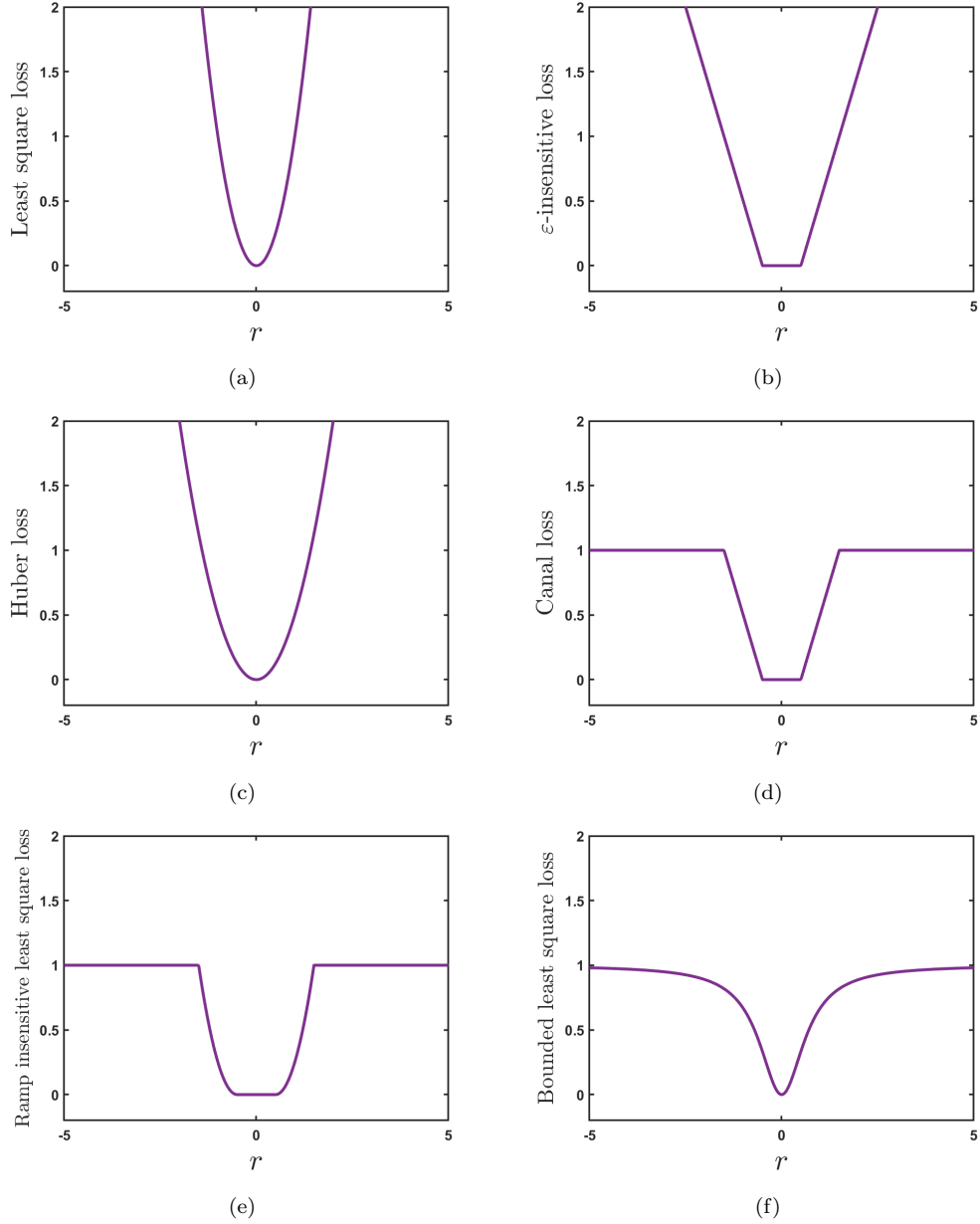


Figure 1: Visual illustration of some baseline loss functions. (a) Least square loss function. (b) ε -insensitive loss function with $\varepsilon = 0.5$. (c) Huber loss function with $\theta = 5$. (d) Canal loss function with $\varepsilon = 0.5$ and $\theta = 1.5$. (e) Ramp insensitive least square loss function with $\varepsilon = 0.5$ and $\theta = 1.5$. (f) Bounded least square loss function with $t = 1$ and $\theta = 2$.

2.1. Unbounded loss functions

The least squares loss function stands as the dominant choice in the realm of regression, characterized by its smoothness and quadratic growth as the regression error escalates. Its widespread application spans across diverse domains [29, 30], with least squares support vector regression (LS-SVR) [17] representing a notable and successful adaptation. However, its rapid growth rate renders it sensitive to the presence of noise in the data [31]. In contrast to least squares loss, the absolute loss function [32] and pinball loss function [33] exhibit linear growth as errors increase and are robust against noise. Nevertheless, these loss functions lack the desirable smoothness property, which can pose challenges for optimization and may lead to slower convergence during model training. Encouragingly, the Huber loss function [18] offers a promising middle ground. It amalgamates the attributes of least squares and absolute loss functions, making it smooth and featuring a relatively gentle growth rate. This characteristic allows it to impose linear penalties on large errors and quadratic penalties on smaller errors. The Huber loss function is widely used due to its balance between robustness and smoothness. Furthermore, numerous extensions of the Huber loss function [34, 35] have been developed, extending its versatility in various applications. In the aforementioned loss functions, all training data points contribute to the regression, often leading to models with reduced sparsity. In contrast, the ε -insensitive loss function takes a different approach by not penalizing data points that fall within an ε -tube around the target values. This offers an element of flexibility and sparsity in the model. While these diverse loss functions have demonstrated significant success in regression, it's imperative to acknowledge their inherent unbounded nature, which renders the corresponding regressors susceptible to the influence of noise and outliers with substantial deviations.

2.2. Bounded loss functions

In the pursuit of creating more robust models capable of withstanding the impact of noise, several bounded loss functions have been proposed in the literature. One prominent example is the ramp loss function, originally developed for classification and later adapted for regression [21]. It imposes a strict limit on the maximum allowable loss for data points with substantial deviations. This approach effectively prevents noise and outliers from exerting an excessive influence, contributing to the model's robustness. Various variations of the ramp loss function, tailored for regression, have been proposed in the literature. The ramp ε -insensitive loss function [36] is a

notable example in this category. It assigns zero penalties to data points with minor errors, while significant errors are met with finite penalties. This well-calibrated design achieves a delicate equilibrium between enhancing robustness and preserving model sparsity. To further emphasize the penalty applied to non-outlier observation errors, the non-convex least squares loss function [22] and the ramp ε -insensitive least squares loss function [37] are introduced in the literature. These incarnations replace the linearly increasing segment of the ramp loss function with a squared form. In recent developments, Ye et al. [25] and Liang et al. [26] respectively proposed the quadratic non-convex insensitive loss function and the canal loss function which are also tailored to address the challenges posed by noisy labels by enforcing a fixed loss on data points with notable deviations. However, it's crucial to acknowledge that most of the aforementioned discussed loss functions adopt the hard truncation strategy which imparts a non-smooth character to these loss functions.

3. Proposed work

In this section, we propose a novel loss function named HawkEye loss, and leveraging this breakthrough, we incorporate the proposed HawkEye loss function into the least squares framework of SVR and yield a new fast and robust support vector regression model coined as HE-LSSVR.

3.1. HawkEye loss function

We present a noteworthy breakthrough in the field of supervised learning: a novel symmetric loss function, termed the HawkEye loss function. It is designed to manifest desirable attributes of boundedness and smoothness while concurrently incorporating an insensitive zone. This innovative approach marks a substantial advancement in optimizing the training process of machine learning models. The mathematical expression of the proposed HawkEye loss function is articulated as follows:

$$\mathcal{L}_{HE}(r, a, \lambda) = \begin{cases} \lambda [1 - \{-a(r + \varepsilon) + 1\}e^{a(r+\varepsilon)}], & r \leq -\varepsilon, \\ 0, & -\varepsilon < r < \varepsilon, \\ \lambda [1 - \{a(r - \varepsilon) + 1\}e^{-a(r-\varepsilon)}], & r \geq \varepsilon, \end{cases} \quad (3)$$

where $\varepsilon > 0$ is an insensitivity parameter that serves to establish a zone of tolerance within the loss function, $a \in \mathbb{R}^+$ is a shape parameter that de-

termines the curvature and steepness of the loss function, and $\lambda \in \mathbb{R}^+$ is a bounding parameter that acts as a constraint to ensure that the loss does not exceed a specified bound. To visually depict the proposed HawkEye loss function (3), Figures 2a and 2b showcase its representation for various combinations of the parameters a and λ . The Proposed HawkEye loss function (3), as delineated in this work, exhibits the following intrinsic properties:

Property 1: $\mathcal{L}_{HE}(\cdot)$ exhibits sparsity, meaning it assigns zero loss to data points falling within a specified ε -insensitive zone.

Proof. For $-\varepsilon < r < \varepsilon$, the loss function $\mathcal{L}_{HE}(\cdot)$ is defined as $\mathcal{L}_{HE}(r) = 0$. This demonstrates that within the ε -insensitive zone, the loss is indeed zero, proving the sparsity property. \square

Property 2: $\mathcal{L}_{HE}(\cdot)$ is symmetric, signifying its impartial allocation of equal loss to deviations on both sides of the reference point.

Proof. Consider two values r and $-r$. From (3), we can easily show that:

$$\mathcal{L}_{HE}(r) = \mathcal{L}_{HE}(-r).$$

This symmetry property is a direct consequence of the construction of the loss function. \square

Property 3: $\mathcal{L}_{HE}(\cdot)$ is non-negative, ensuring that the loss is always greater than or equal to zero.

Proof. For all values of r , the loss function $\mathcal{L}_{HE}(\cdot)$ is defined as a combination of terms that are non-negative:

$$\begin{aligned} \mathcal{L}_{HE}(r) &= \lambda [1 - \{-a(r + \varepsilon) + 1\}e^{a(r+\varepsilon)}], r \leq -\varepsilon, \\ \mathcal{L}_{HE}(r) &= 0, -\varepsilon < r < \varepsilon, \\ \mathcal{L}_{HE}(r) &= \lambda [1 - \{a(r - \varepsilon) + 1\}e^{-a(r-\varepsilon)}], r \geq \varepsilon. \end{aligned}$$

It can be seen easily that all the terms in the definition of $\mathcal{L}_{HE}(\cdot)$ are non-negative, ensuring the non-negativity property. \square

Property 4: $\mathcal{L}_{HE}(\cdot)$ is zero at origin and increases monotonically with respect to $|r|$, i.e., $\mathcal{L}_{HE}(0) = 0$ and $\frac{\partial \mathcal{L}_{HE}}{\partial |r|} \geq 0$.

Proof. Since $\varepsilon > 0$, the origin will always lie in the region $-\varepsilon < r < \varepsilon$. Then, from (3), we can easily see that $\mathcal{L}_{HE}(0) = 0$. Now, to prove that the HawkEye loss function increases monotonically with respect to $|r|$, let's analyze each region separately.

For $r \leq -\varepsilon$:

We can write $\mathcal{L}_{HE}(|r|) = \lambda [1 - \{-a(-|r| + \varepsilon) + 1\}e^{a(-|r|+\varepsilon)}]$.

Taking the derivative with respect to $|r|$, we get:

$$\frac{\partial \mathcal{L}_{HE}}{\partial |r|} = -\lambda a^2(-|r| + \varepsilon)e^{a(-|r|+\varepsilon)}.$$

Since $\lambda, a > 0$, $-|r| + \varepsilon \leq 0$, and $e^{a(-|r|+\varepsilon)}$ is always positive, then we can surely say that the derivative is always non-negative.

For $-\varepsilon < r < \varepsilon$:

In this region, the HawkEye loss function is constant, so $\frac{\partial \mathcal{L}_{HE}}{\partial |r|} = 0$.

For $r \geq \varepsilon$:

We can write $\mathcal{L}_{HE}(|r|) = \lambda [1 - \{a(|r| - \varepsilon) + 1\}e^{-a(|r|-\varepsilon)}]$.

Taking the derivative with respect to $|r|$, we get:

$$\frac{\partial \mathcal{L}_{HE}}{\partial |r|} = \lambda a^2(|r| - \varepsilon)e^{-a(|r|-\varepsilon)}.$$

Since $\lambda, a > 0$, $|r| - \varepsilon \geq 0$, and $e^{-a(|r|-\varepsilon)}$ is always positive, then the derivative is always non-negative.

In conclusion, the HawkEye loss function increases monotonically with respect to $|r|$, i.e., $\frac{\partial \mathcal{L}_{HE}}{\partial |r|} \geq 0$. □

Property 5: $\mathcal{L}_{HE}(\cdot)$ is bounded by λ , ensuring that the loss does not grow unbounded as the error increases, thereby enhancing robustness.

Proof. For this, we analyze its behavior in the three defined regions.

For $r \leq -\varepsilon$:

In this region, we have:

$$\mathcal{L}_{HE}(r) = \lambda [1 - \{-a(r + \varepsilon) + 1\}e^{a(r+\varepsilon)}]. \quad (4)$$

To prove that $\mathcal{L}_{HE}(r)$ is bounded by λ , we need to show that the expression in the square bracket of equation (4) is less than or equal to 1, i.e., $\{-a(r + \varepsilon) + 1\}e^{a(r+\varepsilon)} \geq 0$.

Let's simplify the expression.

$e^{a(r+\varepsilon)}$ is a positive term.

$-a(r + \varepsilon) + 1 \geq 0$ (since $a > 0$ and $r \leq -\varepsilon$).

Thus, the expression in the square bracket of equation (4) is less than or equal to 1. Therefore, in this region, $\mathcal{L}_{HE}(r)$ is bounded by λ .

For $-\varepsilon < r < \varepsilon$:

In this region, we have $\mathcal{L}_{HE}(r) = 0$, which is trivially bounded by λ .

For $r \geq \varepsilon$:

Similar to the first region, we can easily demonstrate that in this region $\mathcal{L}_{HE}(r)$ is also bounded by λ .

Hence, in all three regions, we have shown that $\mathcal{L}_{HE}(r)$ is bounded by λ for the specified parameter values $a > 0$, $\lambda > 0$, and $\varepsilon > 0$. \square

Property 6: $\mathcal{L}_{HE}(\cdot)$ is smooth, indicating that it is differentiable and suitable for gradient-based optimization algorithms.

Proof. The loss function $\mathcal{L}_{HE}(\cdot)$ is meticulously constructed by combining continuous functions and exponential terms, ensuring its overall differentiability. Nevertheless, to dispel any concerns regarding its differentiability specifically at $r = \varepsilon$ and $r = -\varepsilon$, we provide a thorough demonstration limited to these particular points.

At $r = \varepsilon$:

$$\begin{aligned} \text{L.H.D.} &= \lim_{h \rightarrow 0} \frac{\mathcal{L}_{HE}(\varepsilon - h) - \mathcal{L}_{HE}(\varepsilon)}{-h} \\ &= \lim_{h \rightarrow 0} \frac{0 - 0}{-h} && \text{(Using equation (3))} \\ &= 0. \end{aligned}$$

$$\begin{aligned}
\text{R.H.D.} &= \lim_{h \rightarrow 0} \frac{\mathcal{L}_{HE}(\varepsilon + h) - \mathcal{L}_{HE}(\varepsilon)}{h} \\
&= \lim_{h \rightarrow 0} \frac{\lambda [1 - \{a(\varepsilon + h - \varepsilon) + 1\}e^{-a(\varepsilon+h-\varepsilon)}] - 0}{h} \quad (\text{Using equation (3)}) \\
&= \lim_{h \rightarrow 0} \frac{\lambda [1 - \{ah + 1\}e^{-ah}]}{h} \quad \left(\frac{0}{0} \text{ form}\right) \\
&= \lim_{h \rightarrow 0} -\lambda [-a(ah + 1)e^{-ah} + ae^{-ah}] \quad (\text{Using L'hospital rule}) \\
&= -\lambda [-a + a] \\
&= 0.
\end{aligned}$$

Thus, at $r = \varepsilon$, the left-hand derivative and right-hand derivative are both equal. Hence, $\mathcal{L}_{HE}(\cdot)$ is differentiable at $r = \varepsilon$.

At $r = -\varepsilon$:

$$\begin{aligned}
\text{L.H.D.} &= \lim_{h \rightarrow 0} \frac{\mathcal{L}_{HE}(-\varepsilon - h) - \mathcal{L}_{HE}(-\varepsilon)}{-h} \\
&= \lim_{h \rightarrow 0} \frac{\lambda [1 - \{-a(-\varepsilon - h + \varepsilon) + 1\}e^{a(-\varepsilon-h+\varepsilon)}] - 0}{-h} \quad (\text{Using equation (3)}) \\
&= \lim_{h \rightarrow 0} \frac{\lambda [1 - \{-a(-h) + 1\}e^{a(-h)}]}{-h} \quad \left(\frac{0}{0} \text{ form}\right) \\
&= \lim_{h \rightarrow 0} \lambda [-a(ah + 1)e^{-ah} + ae^{-ah}] \quad (\text{Using L'hospital rule}) \\
&= \lambda [-a + a] \\
&= 0.
\end{aligned}$$

$$\begin{aligned}
\text{R.H.D.} &= \lim_{h \rightarrow 0} \frac{\mathcal{L}_{HE}(-\varepsilon + h) - \mathcal{L}_{HE}(-\varepsilon)}{h} \\
&= \lim_{h \rightarrow 0} \frac{0 - 0}{h} \quad (\text{Using equation (3)}) \\
&= 0.
\end{aligned}$$

Thus, at $r = -\varepsilon$, the left-hand derivative and right-hand derivative are both equal. Hence, $\mathcal{L}_{HE}(\cdot)$ is differentiable at $r = -\varepsilon$. Consequently, we have established that $\mathcal{L}_{HE}(\cdot)$ is differentiable throughout its domain. \square

To enable gradient-based optimization, we can derive the derivative of

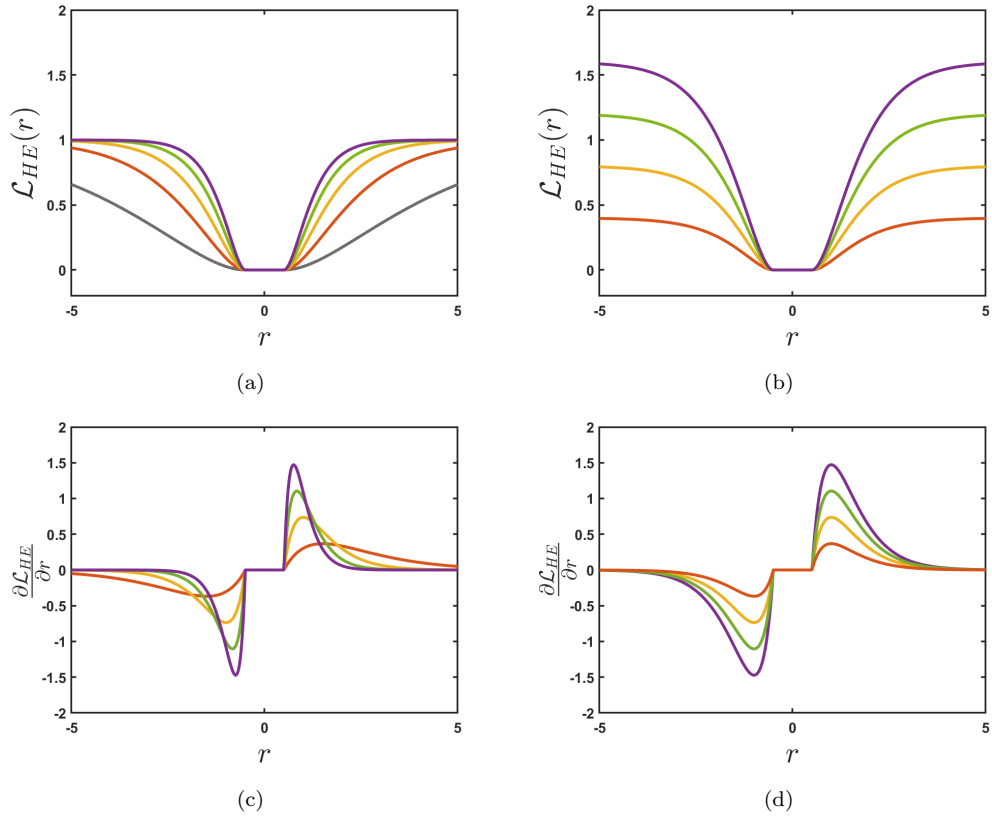


Figure 2: The proposed HawkEye loss function and its gradient for different values of a and λ . Subfigures (a), (c) are plotted for fixed λ and different values of a while (b), (d) are plotted for fixed a and different values of λ .

$\mathcal{L}_{HE}(\cdot)$ with respect to r :

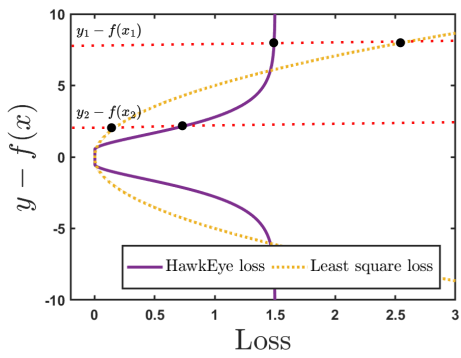
$$\frac{\partial \mathcal{L}_{HE}(r, a, \lambda)}{\partial r} = \begin{cases} \lambda a^2 (r + \varepsilon) e^{a(r+\varepsilon)}, & r < -\varepsilon, \\ 0, & -\varepsilon \leq r \leq \varepsilon, \\ \lambda a^2 (r - \varepsilon) e^{-a(r-\varepsilon)}, & r > \varepsilon. \end{cases} \quad (5)$$

The derivative of $\mathcal{L}_{HE}(\cdot)$ is visualized for different values of parameters in Figures 2c and 2d. The shape of the derivative provides valuable insights into our loss function and its behavior during minimization using gradient descent or some related method. For all values of a and λ , the derivative is 0 when $|r| \leq \varepsilon$, indicating no sensitivity to minor residuals. However, as the magnitude of the residual exceeds ε , the derivative increases with the growth of a and λ . Further, as the magnitude of the residual progressively increases beyond a certain threshold, the magnitude of the derivative begins to decrease, ultimately converging towards zero. Consequently, as the magnitude of an outlier’s residual grows, its influence on the gradient descent process diminishes, and once it surpasses a certain threshold, the outlier’s impact becomes nearly negligible.

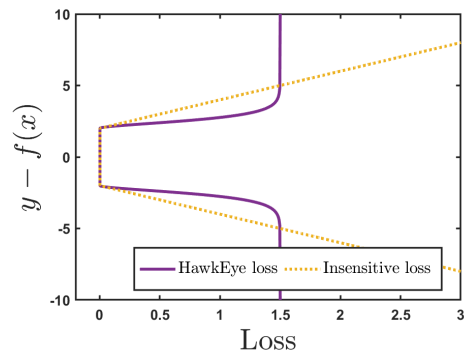
3.2. Comparative Analysis of HawkEye Loss Function with baseline loss functions:

In this subsection, we conduct a comparative analysis of the proposed HawkEye loss function with some established baseline loss functions. Each baseline loss function is examined individually to highlight its characteristics and performance relative to the HawkEye loss function. For the sake of clarity, we presented visual depictions in Figure 3.

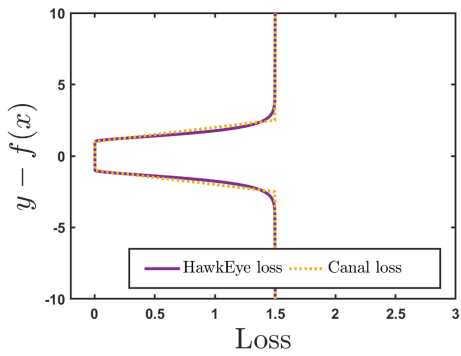
1. **HawkEye loss (\mathcal{L}_{HE}) vs Least square loss (\mathcal{L}_{ls}):** Consider a data point (x_1, y_1) with a noisy label where the target value y_1 is mislabeled for some reason. As a consequence, the target value y_1 deviates significantly from the actual model prediction $f(x_1)$, resulting in a large absolute difference of $|y_1 - f(x_1)|$. In such cases, the least squares loss becomes exceedingly large, and minimizing this loss would have a notorious repercussion on the overall performance of the model. In contrast, when we apply the HawkEye loss to such a data point in similar circumstances, it tends to approach a constrained value, and we note that $\mathcal{L}_{HE}(x_1)$ is notably less than $\mathcal{L}_{ls}(x_1)$ (see Figure 3a). This



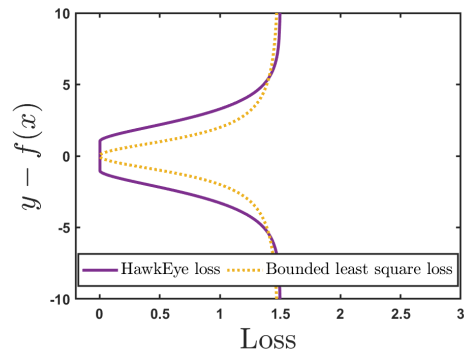
(a)



(b)



(c)



(d)

Figure 3: Visual comparison of HawkEye loss and baseline loss functions. Subfigures (a), (b), (c), and (d) demonstrate the comparison of HawkEye loss function with the least square loss, insensitive loss, canal loss, and bounded least square loss, respectively.

observation underscores that the HawkEye loss function effectively mitigates the influence of noisy data points, highlighting its robustness in the presence of such outliers. Now, let's turn our attention to another data point (x_2, y_2) that is clean and exhibits a small absolute difference $|y_2 - f(x_2)|$. Such points are inherently more amenable to misestimation and thus warrant closer attention. Notably, when we examine the least squares loss for this point, it is less than the corresponding HawkEye loss, as evidenced by $\mathcal{L}_{HE}(x_2) > \mathcal{L}_{ls}(x_2)$. Thus, it can be confidently asserted that, with appropriately selected parameters, the HawkEye loss function not only demonstrates resilience in the presence of noisy data points but also exhibits a capacity for affording greater attention to clean, non-outlier data points.

2. **HawkEye loss (\mathcal{L}_{HE}) vs Insensitive loss (\mathcal{L}_ε):** Similar to the least squares loss function, the insensitive loss function imposes a substantial penalty on samples exhibiting large deviations, making it less robust in the presence of outliers when compared to the HawkEye loss. Furthermore, for a judiciously chosen parameter value, the HawkEye loss exhibits a propensity to allocate greater emphasis to non-outlier points compared to the insensitive loss function. It is also important to highlight that the HawkEye loss function surpasses the insensitive loss function in terms of smoothness. The inherent smoothness property of the HawkEye loss is an added advantage in optimization processes.
3. **HawkEye loss (\mathcal{L}_{HE}) vs Canal loss (\mathcal{L}_{canal}):** The Canal loss is characterized by its capability to constrain the loss to a predefined value through the selection of parameters θ and ε . Similarly, the HawkEye loss function shares this property, as it determines an upper bound λ for penalty and restricts the loss to stop raising after a certain deviation. However, in the context of non-outlier data points, the canal loss maintains a fixed shape. In contrast, the proposed HawkEye loss function exhibits greater versatility, as it can adapt its shape to suit diverse situations by adjusting the shape parameter value a . It's also essential to underscore that the HawkEye loss outshines the canal loss not only in adaptability but also in terms of smoothness. Hence the HawkEye loss, with its smooth profile, presents a more advantageous characteristic compared to the canal loss.
4. **HawkEye loss (\mathcal{L}_{HE}) vs Bounded least square loss (\mathcal{L}_{bls}):** The bounded least square loss function is equipped with the capability to confine the loss within a predefined threshold by adjusting the pa-

Table 2: Demonstrate the characteristics of baseline loss functions used in regression and the proposed HawkEye loss.

Loss function ↓ \ Characteristics →	Robust	Insensitive zone	Bounded	Convex	Smooth
Least square loss	✗	✗	✗	✓	✓
Absolute loss	✗	✗	✗	✓	✗
Huber loss	✗	✗	✗	✓	✓
Insensitive loss	✗	✓	✗	✓	✗
Ramp insensitive loss	✓	✓	✓	✗	✗
Non-convex least square loss	✓	✗	✓	✗	✗
Ramp insensitive least square loss	✓	✓	✓	✗	✗
Quadratic non-convex insensitive loss	✓	✓	✓	✗	✗
Canal loss	✓	✓	✓	✗	✗
Bounded least square loss	✓	✗	✓	✗	✓
HawkEye loss (Proposed)	✓	✓	✓	✗	✓

parameter t . Simultaneously, it offers the flexibility to adapt its shape for non-outlier data points through the modulation of the parameter θ . Intriguingly, the HawkEye loss function also shares both of these remarkable characteristics. A notable highlight is that the HawkEye loss introduces an additional dimension by incorporating the concept of an insensitive zone. An enlightening point of distinction lies in the fact that the HawkEye loss function is the first loss function in SVR literature that not only possesses the attributes of smoothness and boundedness but also concurrently exhibits an insensitive zone.

We have also summarized the key attributes of the existing baseline loss functions and the proposed HawkEye loss function in Table 2.

3.3. SVR with HawkEye loss function

In this subsection, we incorporate the newly proposed HawkEye loss function into the least squares framework of SVR and establish a novel support vector regressor that manifests robustness against outliers and desirable smoothness characteristics. We refer to this advanced regressor as the HE-LSSVR. For the sake of simplicity and without loss of generality, we use the terminology w for $[w^\top, b]$ and x_i for $[x_i, 1]^\top$ throughout the paper. The formulation of the proposed HE-LSSVR is given as:

$$\begin{aligned}
 \min_{w, \xi} \quad & \frac{1}{2} \|w\|^2 + C \sum_{i=1}^N \mathcal{L}_{HE}(\xi_i), \\
 \text{subject to} \quad & \xi_i = y_i - (w^\top \phi(x_i)), \quad \forall i = 1, 2, \dots, N,
 \end{aligned} \tag{6}$$

where $\frac{1}{2}\|w\|^2$ is the regularizer term, $\sum_{i=1}^N \mathcal{L}_{HE}(\xi_i)$ is the empirical risk corresponds to the proposed HawkEye loss function, $C > 0$ is a regularization parameter, ξ_i indicates the regression error of i^{th} input, and $\phi(\cdot)$ represents the high-dimensional feature mapping associated with the kernel function. Let us assume that $\mathcal{K} : \mathbb{R}^m \times \mathbb{R}^m \rightarrow \mathbb{R}$ is a Mercer kernel and $H_{\mathcal{K}}$ is a reproducing kernel Hilbert space induced by \mathcal{K} . In practice, kernel functions are often employed to address nonlinear problems by formulating the relevant dual problems. However, due to the non-convex nature of equation (6), this approach can be quite formidable in our scenario. In this case, to enhance the capacity of HE-LSSVR for nonlinear adaptation, we use the representer theorem [38], which allows us to express w in equation (6) as follows:

$$w = \sum_{k=1}^N \alpha_k \phi(x_k), \quad (7)$$

where $\alpha = (\alpha_1, \dots, \alpha_N)^T$ is the coefficient vector. We note that the minimization problem (6) works in a reproducing kernel Hilbert space, and the penalty term is non-decreasing, so one can apply the representer theorem to the optimization problem (6).

Substituting the value of w from (7) into (6), the primal optimization problem (6) can be transformed into the following unconstrained optimization problem:

$$\min_{\alpha} \sum_{i=1}^N \sum_{k=1}^N \frac{1}{2} \alpha_i \alpha_k \mathcal{K}(x_i, x_k) + C \sum_{i=1}^N \mathcal{L}_{HE}(\xi_i), \quad (8)$$

where $\xi_i = y_i - \sum_{k=1}^N \alpha_k \mathcal{K}(x_i, x_k)$ and $\mathcal{K}(x_i, x_k) = \phi(x_i) \cdot \phi(x_k)$ is the kernel function.

3.4. Adaptive moment estimation (Adam) algorithm for HE-LSSVR

The smoothness characteristic of the non-convex HE-LSSVR model enables the utilization of gradient-based algorithm to optimize the model (8). Leveraging gradient-based optimization offers several advantages, notably expediting convergence during the training process. This is particularly valuable since gradient-based algorithms typically exhibit faster convergence compared to quadratic programming solvers [39]. In this paper, we employ the

adaptive moment estimation (Adam) [40] optimization technique to address the HE-LSSVR problem (8). It effectively combines the strengths of two popular optimization algorithms, AdaGrad [41] and RMSProp [42]. There are mainly three reasons to adopt Adam algorithm. Firstly, Adam employs adaptive learning rates for each weight parameter. This adaptability ensures that the learning rate is neither too high, which could lead to convergence issues, nor too low, which could slow down convergence. Thus contributing to faster and more stable convergence. Secondly, Adam incorporates the concept of momentum, which improves convergence in complex optimization landscapes. By maintaining a moving average of past gradients, it navigates these landscapes more efficiently and accelerates the convergence process. Finally, Adam utilizes exponentially decreasing averages for previous gradients and squared gradients, providing flexibility to adapt to changing gradient behavior. This feature is well-suited for non-convex optimization tasks, where gradient characteristics may vary significantly throughout the training process.

Now, to begin with, let the objective function of (8) be $H(\alpha)$. Then, the procedure for applying the Adam algorithm is as follows:

1. **Initialization:** Start by initializing the algorithm with appropriate values for hyperparameters:
 Learning Rate (γ): This is the step size for updating model parameters. β_1 and β_2 : These are constants for computing moving averages of gradients and squared gradients. δ : A small constant added to prevent division by zero.
2. **Initialize Moments:** Initialize the values of the first moment estimate (m) and the second moment estimate (v). These moments are used to keep track of past gradients and squared gradients, respectively.
3. **Iterative Optimization:** At each iteration t :
 - Compute the gradient of the objective function $H(\alpha)$ with respect to the model parameters α .

$$\nabla H(\alpha_t) = \mathcal{K}\alpha + C \sum_{i=1}^N \frac{\partial \mathcal{L}_{HE}}{\partial \alpha}, \quad (9)$$

where

$$\frac{\partial \mathcal{L}_{HE}}{\partial \alpha} = \begin{cases} -\lambda a^2 (\xi_i + \varepsilon) e^{a(\xi_i + \varepsilon)} \mathcal{K}_i, & \xi_i < -\varepsilon, \\ 0, & -\varepsilon \leq \xi_i \leq \varepsilon, \\ -\lambda a^2 (\xi_i - \varepsilon) e^{-a(\xi_i - \varepsilon)} \mathcal{K}_i, & \xi_i > \varepsilon. \end{cases}$$

Here \mathcal{K}_i represent the i^{th} row of the kernel matrix \mathcal{K} .

- Update the first moment estimate:

$$m_t = \beta_1 m_{t-1} + (1 - \beta_1) \nabla H(\alpha_t). \quad (10)$$

- Update the second moment estimate:

$$v_t = \beta_2 v_{t-1} + (1 - \beta_2) \nabla H(\alpha_t)^2. \quad (11)$$

- Correct the bias in moments (due to initialization):

$$\hat{m}_t = \frac{m_t}{(1 - \beta_1^t)}, \quad (12)$$

$$\hat{v}_t = \frac{v_t}{(1 - \beta_2^t)}. \quad (13)$$

- Update model parameter:

$$\alpha_t = \alpha_{t-1} - \gamma \frac{\hat{m}_t}{\sqrt{\hat{v}_t + \delta}}. \quad (14)$$

4. **Convergence Criterion:** Monitor the convergence of the optimization process. A common stopping criterion is a maximum number of iterations or a target value for the objective function $H(\alpha)$.
5. **Termination:** When the algorithm meets the convergence criterion, terminate the optimization process, and the final model parameters α represent the optimal solution for the problem $H(\alpha)$.

The structure of the Adam algorithm to solve the HE-LSSVR model is clearly described in Algorithm 1. Once the optimal α is obtained, the following decision function can be utilized to predict the target value of a new sample

x .

$$f(x) = \sum_{k=1}^N \alpha_k \mathcal{K}(x, x_k). \quad (15)$$

For delineating the intricacies of the proposed HE-LSSVR model, in Figure 4, we present a meticulously crafted flowchart that captures the essence of our methodology. This visual narrative serves not only as a roadmap for our methodology but also as a testament to the strategic interplay of components that positions HE-LSSVR as a cutting-edge regression model.

Algorithm 1 Adam algorithm for HE-LSSVR

Input:

The dataset: $\{x_i, y_i\}_{i=1}^N$, $y_i \in \mathbb{R}$;

The parameters: Regularization parameter C , HawkEye loss parameters λ , a , and ε , mini-batch size s , decay rates β_1 and β_2 , learning rate γ , constant δ , maximum iteration number T ;

Initialize: α_0 and t ;

Output:

The classifiers parameters: α ;

1 : Select s samples $\{x_i, y_i\}_{i=1}^s$ uniformly at random.

2 : Computing ξ_i :

$$\xi_i = y_i - \sum_{k=1}^s \alpha_k \mathcal{K}(x_i, x_k), \quad i = 1, \dots, s; \quad (16)$$

3 : Compute $\nabla H(\alpha_t)$: (9);

4 : Compute m_t : (10);

5 : Compute v_t : (11);

6 : Compute \hat{m}_t : (12);

7 : Compute \hat{v}_t : (13);

8 : Updating solution α_t : (14);

9 : Updating current iteration number: $t = t + 1$.

Until:

$t = T$

Return: α_t .

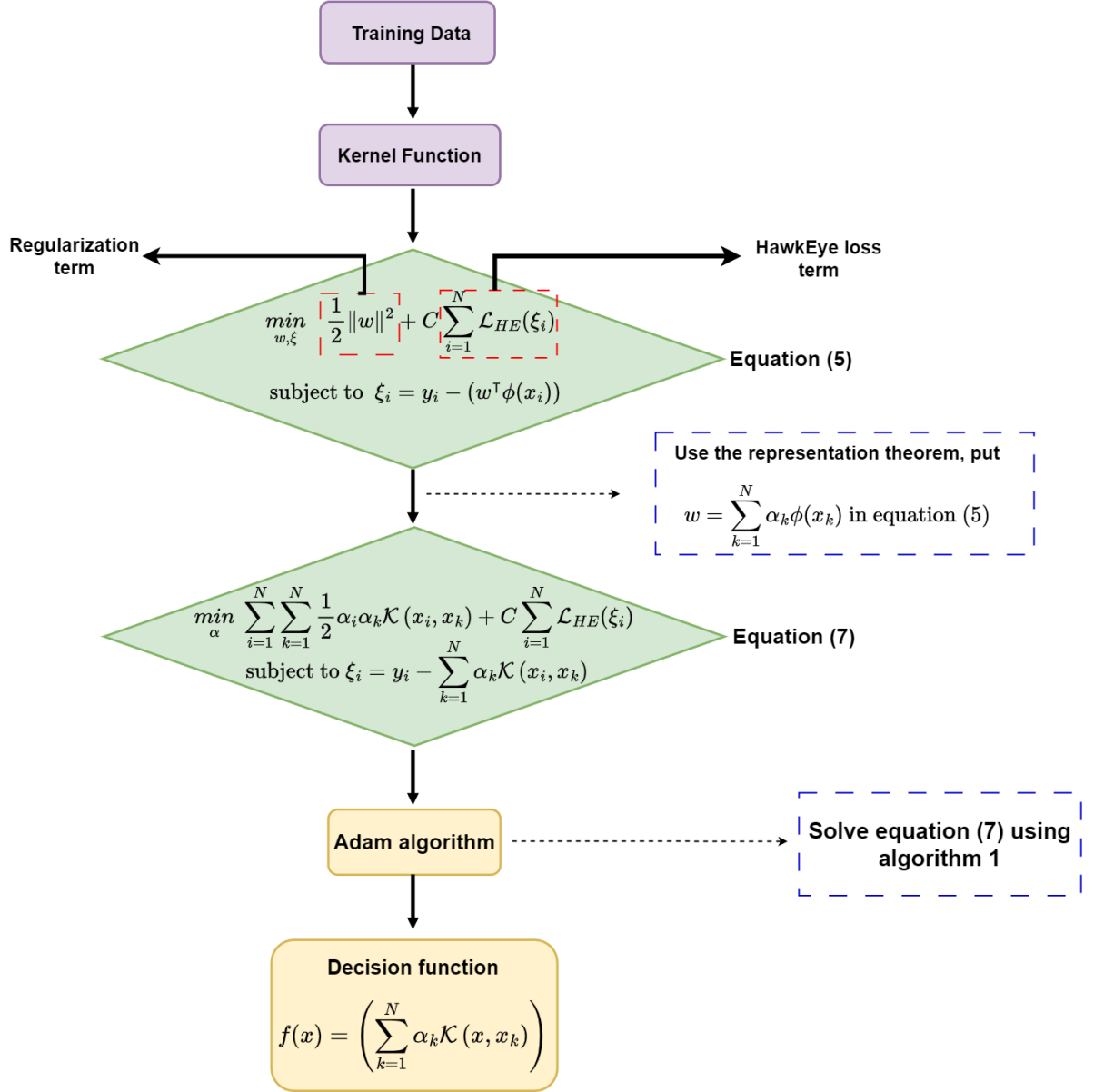


Figure 4: Flowchart illustrating the key stages of the HE-LSSVR model, showcasing the transformation from original input data to the decision function, highlighting the strategic integration of the HawkEye loss function and the application of representer theorem and Adam algorithm.

4. Numerical Experiments and Result Analysis

In this section, we conduct extensive experiments on UCI, syntetic and time series datasets to compare the proposed HE-LSSVR model with existing state-of-the-art models, which include support vector regression (SVR) [4], least squares support vector regression (LS-SVR) [17], and bounded least squares support vector regression (BLSSVR) [43].

4.1. Experimental Setup and Parameter Setting

All the experiments are executed using MATLAB R2023a on Window 10 running on a PC with configuration Intel(R) Xeon(R) Gold 6226R CPU @ 2.90GHz, 2901 Mhz, 16 Core(s), 32 Logical Processor(s) with 128 GB of RAM. The kernel function plays a pivotal role in addressing non-linear models. We use the radial basis function (RBF) kernel as it is widely recognized for its high performance in regression tasks [44]. The RBF kernel is defined as $\mathcal{K}(x_i, x_k) = \exp(-\|x_i - x_k\|^2 / \sigma^2)$, where σ is an adjustable parameter. For each model, the regularization parameter C and kernel parameter σ are selected from the set $\{10^i \mid i = -6, -4, \dots, 4, 6\}$. For SVR and the proposed HE-LSSVR, the insensitive zone parameter ε is selected from the set $\{0.001, 0.005, 0.01, 0.05, 0.1, 0.15, 0.2, 0.25\}$. The loss hyperparameters for BLSSVR are adopted the same as in [43]. For the proposed HE-LSSVR, loss hyperparameters λ and a are selected from the ranges $[0.1 : 0.2 : 2]$ and $[0.1 : 0.2 : 5]$, respectively. The Adam algorithm parameters are empirically configured as follows: (i) initial model parameter $\alpha_0 = 0.01$, (ii) initial first moment $m_0 = 0.01$, (iii) initial second moment $v_0 = 0.01$, (iv) initial learning rate γ is chosen from the set $\{0.0001, 0.001, 0.01\}$, (v) exponential decay rate of first order $\beta_1 = 0.9$, (vi) exponential decay rate of second order $\beta_2 = 0.999$, (vii) division constant $\delta = 10^{-8}$, (viii) mini-batch size $s = 2^5$, (x) maximum iteration number $T = 1000$.

The performance of machine learning models is markedly affected by the choice of hyperparameters [45]. To optimize these hyperparameters effectively, we performed a tuning process using k -fold ($k = 5$) cross-validation and grid search. This procedure involved dividing the dataset into five distinct and non-overlapping subsets, commonly referred to as “folds”. During each iteration, one of these subsets is designated for testing purposes, while the remaining four are employed for training. For each distinct set of hyperparameters, we computed the root mean squared error (RMSE) separately on

Table 3: The evaluation metrics.

Metrics	Definitions
RMSE	$\sqrt{\frac{1}{N} \sum_{i=1}^N (y_i - f(\mathbf{x}_i))^2}$
MAE	$\frac{1}{N} \sum_{i=1}^N (y_i - f(\mathbf{x}_i)) $
Error _{pos}	$\frac{1}{N} \sum_{i=1, y_i \geq f(\mathbf{x}_i)}^N y_i - f(\mathbf{x}_i) $
Error _{neg}	$\frac{1}{N} \sum_{i=1, y_i < f(\mathbf{x}_i)}^N y_i - f(\mathbf{x}_i) $

each fold. We then determined the best result for each set of hyperparameters. Finally, one with the lowest RMSE is selected as the optimal parameter combination.

4.2. Evaluation Metrics

Let y_i , $f(x_i)$ represent the actual and predicted values of x_i , respectively. To assess the models' performance, we employ four evaluation metrics: root mean squared error (RMSE), mean absolute error (MAE), positive error (Error_{pos}), and negative error (Error_{neg}). The specific definitions of these metrics are listed in Table 3. We primarily use RMSE as the key comparative measure, while the other metrics serve as supplementary evaluation criteria. Further, to show the efficiency of the proposed BS-SSVR, we also performed a comparative analysis of the training time.

4.3. Experiments on Benchmark UCI Datasets

In this subsection, we use 18 regression benchmark datasets from the UCI repository [46] to assess and compare the performance of the proposed HE-LSSVR against the baseline models. These datasets can be categorized into three groups: 1) 8 small-size datasets with samples ranging from 60 up to 500; 2) 4 medium-size datasets with samples ranging from 501 up to 1000; and 3) 6 large-size datasets with samples ranging from 1001 up to 40768. The detailed description of the datasets is listed in Table 4. The experimental result of the proposed HE-LSSVR model and baseline models (SVR, LS-SVR, and BLSSVR) on UCI datasets in terms of metric RMSE, MAE, Error_{pos},

and Error_{neg} is presented in Table 5. The evaluation is primarily based on the RMSE, a critical metric where lower values indicate superior model performance. The proposed HE-LSSVR model demonstrates noteworthy performance, achieving the best RMSE values on 13 out of 18 datasets. Even on the remaining 5 datasets, HE-LSSVR secures the second-best RMSE. This consistency across a diverse set of datasets underscores the prowess of the HE-LSSVR model. The average RMSE values further validate the effectiveness of HE-LSSVR. The existing SVR, LS-SVR, and BLSSVR models exhibit average RMSE values of 0.3113, 0.6629, and 0.3266, respectively. In contrast, the proposed HE-LSSVR outperforms the baseline models with an average RMSE of 0.2736. To ensure an accurate assessment of the models' performance, it is important to rank them individually for each dataset instead of relying solely on average RMSE. As exceptional performance on certain datasets may overshadow subpar performance on others. Table 6 presents the ranks assigned to each model based on their RMSE values across all datasets. The model with the lowest RMSE receives the lowest rank and vice-versa. The average rank for SVR, LSSVR, BLSSVR, and the proposed HE-LSSVR are 2.5294, 3.8888, 2, and 1.2777, respectively. It clearly demonstrates that the proposed HE-LSSVR model outperforms the baseline models, indicating its superior performance.

To further support the effectiveness of the proposed HE-LSSVR model, we conducted a statistical analysis using the Friedman test, followed by the Nemenyi post hoc test. The Friedman test [47] is utilized to statistically assess the significance of various models. In this test, each individual model is ranked independently for each dataset. The null hypothesis posits that all models are essentially identical, implying that the average rank of each model is equivalent. The Friedman statistic adheres to the chi-squared χ_F^2 distribution with degrees of freedom (d.f.) equal to $p - 1$, where p represents the number of models. This statistic is computed as follows:

$$\chi_F^2 = \frac{12D}{p(p+1)} \left[\sum_e R_e^2 - \frac{p(p+1)^2}{4} \right]. \quad (17)$$

Here, D signifies the total number of datasets, and R_e denotes the mean rank of the e^{th} model out of the p models. However, the Friedman statistic is overly cautious in nature. To address this, Iman and Davenport [48] introduced a

more robust statistic:

$$F_F = \frac{(D-1)\chi_F^2}{D(p-1) - \chi_F^2}, \quad (18)$$

which follows F distribution with $((p-1), (p-1)(D-1))$ d.f.. For $p = 4$ and $D = 18$, we obtain $\chi_F^2 = 23.2540$ and $F_F = 12.8575$. Also, F_F is distributed with $(3, 51)$ d.f.. From the statistical F-distribution table, at 5% level of significance, the value of $F_{(3,51)} = 2.68$. Since, $F_F > 2.68$, thus we reject the null hypothesis. Hence, substantial differences exist among the models. Next, we conduct the Nemenyi post hoc test [49] to compare the models pairwise. The disparity in performance between the two models is considered significant if the corresponding average ranks display a noticeable difference surpassing a specific threshold value known as the critical difference ($C.D.$). When the discrepancy in mean ranks between the two models exceeds the $C.D.$, the model with the higher mean rank is deemed statistically superior to the model with the lower mean rank. The computation of $C.D.$ follows the following formula:

$$C.D. = q_\alpha \sqrt{\frac{p(p+1)}{6D}}. \quad (19)$$

Here, q_α is derived from the studentized range statistic divided by $\sqrt{2}$. This value is referred to as the critical value for the two-tailed Nemenyi test. From the distribution table, at 5% level of significance, the value of q_α is 2.569. Thus, after calculation, we obtain $C.D. = 1.1055$. Table 7 presents the results of the Nemenyi post hoc test on UCI datasets. The average rank differences of the proposed HE-LSSVR from SVR, LS-SVR, and BLSSVR are 1.2517, 2.6103, and 0.7223, respectively. Notably, the disparities in the average ranks for SVR and LSSVR exceed the $C.D.$; thus, according to the Nemenyi post hoc test, the proposed HE-LSSVR is significantly better than SVR and LS-SVR. It is noteworthy that the proposed HE-LSSVR model does not show a statistical difference from the BLSSVR; however, the proposed HE-LSSVR model outperformed the BLSSVR on 16 out of 18 datasets (see Table 5). Considering these results, we can conclude that the HE-LSSVR model exhibits superiority over the baseline models.

To show the efficacy of the proposed HE-LSSVR model in terms of computation, we also evaluated the training time of the models. Table 8 illustrates

the training times for both baseline models and the proposed HE-LSSVR models across different datasets. The 2D_Planes dataset was left out because it had a memory error during training for the SVR model. The average training times for SVR, LS-SVR, BLSSVR, and HE-LSSVR are 34.7984s, 11.7617s, 0.0039s, and 0.0049s, respectively. These results manifest the exceptional efficiency of the proposed HE-LSSVR, with significantly lower training times compared to SVR and LS-SVR. However, the proposed HE-LSSVR takes a slightly longer time to train than the BLSSVR, although the difference in training time is minor. It is crucial to note that the comparative evaluation of RMSE and training time demonstrates the overall performance of the models. In this regard, the proposed HE-LSSVR model stands out as it strikes a balance between RMSE and training time, making it superior to the baseline models.

Table 4: Description of benchmark UCI datasets.

Datasets	No. of samples	No. of features
Airfoil_Self_Noise	1503	5
Delta_Ailerons	7129	5
Forest_Fires	517	12
Yacht_Hydrodynamics	308	6
2D_Planes	40768	10
Ailerons	13750	40
Parkinsons_Telemonitoring	5875	21
Pole_Telecomm	15000	48
2014_2015 CSM dataset	185	11
cpu_pref	209	9
hungary chickenpox	522	19
istanbul stock exchange data	536	8
mcs_ds_edited_iter_shuffled	107	5
qsar_aquatic toxicity	546	8
Daily_Demand_Forecasting_Orders	60	12
bodyfat	252	14
machine	209	9
slump_test	103	10

Table 5: RMSE, MAE, Error_{pos}, and Error_{neg} values on the benchmark UCI datasets for the proposed HE-LSSVR model and the baseline models.

Dataset	Metric	SVR[4]	LS-SVR[17]	BLSSVR[43]	HE-LSSVR [†]
2014.2015 CSM dataset	RMSE	0.2604	0.3564	0.2547	0.2418
	MAE	0.1916	0.3193	0.1674	0.1722
	Error _{pos}	0.2824	0.2588	0.2373	0.2626
	Error _{neg}	0.1625	0.3288	0.1295	0.134
cpu_pref	RMSE	0.0332	0.3907	0.0379	0.0379
	MAE	0.0231	0.3889	0.0298	0.0298
	Error _{pos}	0.0232	-	0.0238	0.0238
	Error _{neg}	0.023	0.3889	0.0395	0.0394
hungary chickenpox	RMSE	0.4892	0.7157	0.487	0.487
	MAE	0.3607	0.6105	0.3484	0.3492
	Error _{pos}	0.4542	0.519	0.4442	0.4517
	Error _{neg}	0.3112	0.627	0.2861	0.2852
istanbul stock exchange data	RMSE	0.5783	0.5798	0.5709	0.5644
	MAE	0.4502	0.4513	0.4443	0.4512
	Error _{pos}	0.4889	0.4835	0.4838	0.5079
	Error _{neg}	0.4054	0.4109	0.3967	0.3378
mcs_ds_edited_iter_shuffled	RMSE	0.1014	0.6715	0.0978	0.0812
	MAE	0.0855	0.5937	0.0796	0.0623
	Error _{pos}	0.0781	0.0189	0.0878	0.0817
	Error _{neg}	0.0974	0.6224	0.0727	0.0342
qsar_aquatic toxicity	RMSE	0.679	0.6224	0.5708	0.5348
	MAE	0.5889	0.4765	0.5055	0.2557
	Error _{pos}	1.1452	1.0737	0.8531	0.2741
	Error _{neg}	0.5135	0.3737	0.45	0.0731
Daily_Demand_Forecasting_Orders	RMSE	0.0426	0.4943	0.0493	0.0424
	MAE	0.0361	0.4919	0.0437	0.0345
	Error _{pos}	0.0307	-	0.0535	0.0259
	Error _{neg}	0.047	0.4919	0.0367	0.0518
bodyfat	RMSE	0.0506	1.1625	0.0567	0.037
	MAE	0.0381	1.0902	0.047	0.0282
	Error _{pos}	0.0559	-	0.0537	0.0265
	Error _{neg}	0.0284	1.0902	0.0422	0.0305
machine	RMSE	0.0329	0.3924	0.0382	0.0382
	MAE	0.0223	0.3893	0.0299	0.0301
	Error _{pos}	0.0223	-	0.0242	0.0254
	Error _{neg}	0.0222	0.3893	0.0383	0.037
slump_test	RMSE	0.0308	0.2741	0.0329	0.0251
	MAE	0.0285	0.2261	0.0286	0.0209
	Error _{pos}	0.0309	0.1493	0.0321	0.0238
	Error _{neg}	0.027	0.2675	0.022	0.0197
Airfoil_Self_Noise	RMSE	0.2286	0.2967	0.2268	0.0864
	MAE	0.1873	0.2702	0.1764	0.0505
	Error _{pos}	0.2617	0.2283	0.2531	0.0699
	Error _{neg}	0.1551	0.279	0.1334	0.0088
Delta_Ailerons	RMSE	0.3653	0.507	0.3637	0.1881
	MAE	0.3026	0.4186	0.3003	0.144
	Error _{pos}	0.2924	0.1732	0.3115	0.1378
	Error _{neg}	0.311	0.4846	0.2895	0.1525

Table 5: (Continued) RMSE, MAE, Error_{pos}, and Error_{neg} values on the benchmark UCI datasets for the proposed HE-LSSVR model and the baseline models.

Dataset	Metric	SVR[4]	LS-SVR[17]	BLSSVR[43]	HE-LSSVR [†]
Forest_Fires	RMSE	0.1487	0.4088	0.1183	0.1183
	MAE	0.0994	0.394	0.0935	0.0936
	Error _{pos}	0.0322	0.6846	0.0653	0.0655
	Error _{neg}	0.1109	0.3883	0.1654	0.1653
Yacht_Hydrodynamics	RMSE	1.0056	1.1753	0.5702	0.5998
	MAE	0.9105	0.8238	0.532	0.4612
	Error _{pos}	1.0019	0.8958	0.5362	0.3786
	Error _{neg}	0.8248	0.2683	0.5309	0.5801
2D_Planes	RMSE	*	2.163	1.4336	1.1251
	MAE	*	1.9962	1.2799	0.9513
	Error _{pos}	*	1.9949	1.0785	1.003
	Error _{neg}	*	1.9973	1.4062	0.8978
Ailerons	RMSE	0.1524	0.1587	0.1195	0.1365
	MAE	0.1461	0.1513	0.107	0.1094
	Error _{pos}	0.1316	0.1714	0.0963	0.1302
	Error _{neg}	0.1654	0.1255	0.1219	0.0426
Parkinsons_Telemonitoring	RMSE	0.0349	0.4306	0.0449	0.0385
	MAE	0.0291	0.4283	0.0379	0.0321
	Error _{pos}	0.0206	-	0.0398	0.033
	Error _{neg}	0.0316	0.4283	0.0362	0.0313
Pole_Telecomm	RMSE	1.0588	1.1328	0.8054	0.5421
	MAE	0.9695	0.9034	0.7546	0.4284
	Error _{pos}	1.378	1.6409	0.8935	0.4653
	Error _{neg}	0.7773	0.5044	0.6924	0.408
Average RMSE		0.3113	0.6629	0.3266	0.2736

[†] represents the proposed model.

The boldface denotes the RMSE of the best model corresponding to each dataset.

* denotes that the Matlab program encounters an “out of memory” error.

Table 6: Rank of RMSE for the proposed HE-LSSVR and baseline models on benchmark UCI datasets.

Dataset	SVR[4]	LS-SVR[17]	BLSSVR[43]	HE-LSSVR [†]
2014_2015_CSM_dataset	3	4	2	1
cpu_pref	1	4	2	2
hungary_chickenpox	3	4	1	1
istanbul_stock_exchange_data	3	4	2	1
mcs_ds_edited_iter_shuffled	3	4	2	1
qsar_aquatic_toxicity	4	3	2	1
Daily_Demand_Forecasting_Orders	2	4	3	1
bodyfat	2	4	3	1
machine	1	4	2	2
slump_test	2	4	3	1
Airfoil_Self_Noise	3	4	2	1
Delta_Ailerons	3	4	2	1
Forest_Fires	3	4	1	1
Yacht_Hydrodynamics	3	4	1	2
2D_Planes	-	3	2	1
Ailerons	3	4	1	2
Parkinsons_Telemonitoring	1	4	3	2
Pole_Telecomm	3	4	2	1
Average Rank	2.5294	3.8888	2	1.2777

Table 7: Difference in the RMSE rankings of the proposed HE-LSSVR model against baseline models on UCI datasets.

Model	Average rank	Rank difference	Significant difference (As per Nemenyi post hoc test)
SVR [4]	2.5294	1.2517	Yes
LS-SVR [17]	3.8888	2.6103	Yes
BLSSVR [43]	2	0.7223	No
HE-LSSVR [†]	1.2777	-	N/A

[†] represents the proposed model.

Table 8: Training time in seconds of the proposed HE-LSSVR model and baseline models on benchmark UCI datasets.

Dataset	SVR[4]	LS-SVR[17]	BLSSVR[43]	HE-LSSVR
2014_2015 CSM dataset	0.0119	0.0042	0.0037	0.0027
cpu_pref	0.0117	0.0046	0.0033	0.0037
hungary chickenpox	0.0925	0.4889	0.0045	0.003
istanbul stock exchange data	0.0657	0.0537	0.0034	0.0031
mcs_ds.edited_iter_shuffled	0.004	0.002	0.0035	0.0032
qsar_aquatic toxicity	0.0839	0.0362	0.0037	0.0029
Daily_Demand_Forecasting_Orders	0.0029	0.001	0.0035	0.0031
bodyfat	0.0136	0.0082	0.0018	0.0044
machine	0.0135	0.0049	0.0041	0.0039
slump_test	0.0069	0.0028	0.0041	0.0033
Airfoil_Self_Noise	0.6113	0.3825	0.004	0.0032
Delta_Ailerons	66.606	24.4937	0.0053	0.0074
Forest_Fires	0.0616	0.0371	0.0037	0.0028
Yacht_Hydrodynamics	0.0177	0.0142	0.0035	0.0112
Ailerons	152.7565	71.5022	0.006	0.0043
Parkinsons_Telemonitoring	24.9768	7.6544	0.0041	0.0103
Pole_Telecomm	346.2366	95.2581	0.0045	0.0115
Average Time	34.7984	11.7617	0.0039	0.0049

4.4. Experiments on Synthetic Datasets

To further analyze and compare the proposed HE-LSSVR with baseline models, in this subsection we construct synthetic datasets with varying levels of noise. A detailed description of the synthetic datasets used for evaluation is provided in Table 9. We have generated five artificial datasets, each of which is duplicated with three different types of noise (Gaussian noise, uniform noise, and student random variable noise), resulting in a total of 15 artificial datasets, each containing 500 samples. Table 10 presents the RMSE values for both the proposed HE-LSSVR model and the baseline models on synthetic datasets. Across the 15 synthetic datasets examined, the proposed HE-LSSVR model outperforms the baseline models on 14 datasets, demonstrating its superior performance in the majority of cases. This observation significantly underscores the robustness and effectiveness of the proposed HE-LSSVR model in comparison to the baseline models.

4.5. Experiments on Time Series Datasets

To validate the superiority of the proposed HE-LSSVR model in real-world applications, we further evaluate it on time series datasets [50]. The

Table 9: Description of synthetic datasets.

Name	Function expression	ϱ	Variable domain
Function 1	$y_i = \sin x_i + \varrho_i$		$x_i \in [0, 2\pi]$
Function 2	$y_i = \frac{\sin(3x_i)}{3x_i} + \varrho_i$		$x_i \in [-4, 4]$
Function 3	$y_i = \sin x_i \cos x_i^2 + \varrho_i$	$\varrho_i \sim N(0, 0.2^2),$ $U[-0.2, 0.2],$ $T(10)$	$x_i \in [0, 2\pi]$
Function 4	$y_i = x_i \cos x_i + \varrho_i$		$x_i \in [-4, 4]$
Function 5	$y_i = (1 - x_i + 2x_i^2) \exp(\frac{-x_i^2}{2}) + \varrho_i$		$x_i \in [-4, 4]$

Here, $N(0, d^2)$ represents the Gaussian random variable with zero mean and standard deviation d . $U[-a, a]$ represents the uniformly random variable in $[-a, a]$. $T(c)$ represents the student random variable with c degree of freedom.

Table 10: RMSE values on the synthetic datasets for the proposed HE-LSSVR model against baseline models.

Dataset	Metric	SVR[4]	LS-SVR[17]	BLSSVR[43]	HE-LSSVR
Type 1: Gaussian noise with 0 mean and 0.2 standard deviation					
Function 1	RMSE	0.12381	0.70565	0.12153	9.84×10^{-6}
Function 2	RMSE	0.0005	0.64655	0.00459	1.93×10^{-5}
Function 3	RMSE	0.09197	0.70557	0.12153	7.59×10^{-6}
Function 4	RMSE	0.00127	0.64479	0.03179	8.52×10^{-5}
Function 5	RMSE	0.00067	0.6585	0.0296	7.34×10^{-5}
Type 2: Uniform noise over the interval $[-0.2, 0.2]$					
Function 1	RMSE	0.07732	0.70559	0.12114	9.84×10^{-6}
Function 2	RMSE	0.00023	0.64655	0.00459	1.93×10^{-5}
Function 3	RMSE	0.0849	0.70555	0.12153	7.59×10^{-6}
Function 4	RMSE	0.00101	0.64162	0.01218	1.58×10^{-5}
Function 5	RMSE	0.00061	0.66018	0.0296	7.27×10^{-5}
Type 3: Student random variable noise with 10 degrees of freedom					
Function 1	RMSE	0.10258	0.7056	0.12153	4.1×10^{-6}
Function 2	RMSE	0.00103	0.64677	0.00459	5.81×10^{-5}
Function 3	RMSE	0.00174	0.68897	0.00319	2.74×10^{-7}
Function 4	RMSE	0.00121	0.64258	0.03179	1.42×10^{-5}
Function 5	RMSE	0.00018	0.6595	0.0296	0.00019

experimental results of the proposed HE-LSSVR and the baseline models are presented in Table 12. The proposed HE-LSSVR showcases remarkable performance as it has the lowest RMSE value on each of the 11 time series datasets. The average RMSE values of the proposed HE-LSSVR and the baseline models (SVR, LS-SVR, and BLSSVR) are 2.2772, 2.6727, 5.2239, and 2.5178, respectively. These values represent the overall performance of each model, with lower RMSE values indicating better predictive accuracy. The results strongly reflect the prominence of the proposed HE-LSSVR model compared to the baseline models.

5. Conclusions and Future work

In this paper, we addressed the limitations of support vector regression (SVR) by introducing the HawkEye loss function, a novel symmetric loss function that is bounded, smooth, and simultaneously possesses an insensitive zone. We presented a comparative analysis of existing loss functions and demonstrated that the HawkEye loss function is the first of its kind in the SVR literature. Further, we integrated the HawkEye loss function into the least squares framework of SVR and developed a new fast and robust model called HE-LSSVR. To solve the optimization problem of HE-LSSVR, we employed the adaptive moment estimation (Adam) algorithm, which offers adaptive learning rates and is effective in handling large-scale problems. This is the first time Adam has been utilized to solve an SVR problem. Through extensive numerical experiments on UCI, synthetic, and time series datasets, we empirically validated the superiority of the proposed HE-LSSVR model. It exhibits remarkable generalization performance and efficiency in training time compared to baseline models. These findings collectively positioned the HE-LSSVR model as a superior choice for real-world applications in diverse fields, affirming its significance and potential impact in the realm of regression tasks.

In the future, there is a potential avenue for delving into the integration of the HawkEye loss function within the domain of deep learning models. The essential characteristics of boundedness and smoothness intrinsic to the HawkEye loss function suggest promising possibilities for its fusion with advanced machine learning and deep learning techniques. This future direction holds the potential to yield substantial advancements and broader applicability across diverse domains.

Table 11: RMSE, MAE, Error_{pos}, and Error_{neg} values on the time series datasets for the proposed HE-LSSVR model against baseline models.

Dataset (No. of samples, No. of features)	Metric	SVR[4]	LS-SVR[17]	BLSSVR[43]	HE-LSSVR [†]
NNGC1_dataset_D1_V1.003 (430, 5)	RMSE	0.6837	0.7501	0.6192	0.5369
	MAE	0.5544	0.593	0.5043	0.4444
	Error _{pos}	0.5957	0.6757	0.5316	0.4377
	Error _{neg}	0.5168	0.4536	0.4715	0.4526
NNGC1_dataset_D1_V1.004 (545, 5)	RMSE	0.562	0.6041	0.4883	0.4221
	MAE	0.4701	0.5045	0.4047	0.3459
	Error _{pos}	0.2759	0.2825	0.4481	0.3219
	Error _{neg}	0.5699	0.5812	0.3764	0.3627
NNGC1_dataset_D1_V1.005 (430, 5)	RMSE	0.0307	0.4047	0.0328	0.0298
	MAE	0.0255	0.4028	0.0274	0.0247
	Error _{pos}	0.025	0.4028	0.0222	0.0252
	Error _{neg}	0.0259	-	0.0301	0.0243
NNGC1_dataset_D1_V1.006 (610, 5)	RMSE	0.1697	0.4305	0.1678	0.1566
	MAE	0.138	0.3945	0.136	0.128
	Error _{pos}	0.1426	0.3967	0.1532	0.1283
	Error _{neg}	0.1337	0.1237	0.1136	0.1277
NNGC1_dataset_D1_V1.007 (610, 5)	RMSE	0.086	0.4104	0.0877	0.0833
	MAE	0.0673	0.4013	0.069	0.065
	Error _{pos}	0.0679	0.4013	0.0639	0.0662
	Error _{neg}	0.0668	-	0.0724	0.0638
NNGC1_dataset_D1_V1.008 (540, 5)	RMSE	0.0982	0.4195	0.0998	0.0949
	MAE	0.0773	0.4078	0.0762	0.075
	Error _{pos}	0.0693	0.4078	0.0585	0.0718
	Error _{neg}	0.0868	-	0.0939	0.0789
NNGC1_dataset_D1_V1.009 (540, 5)	RMSE	0.2481	0.44	0.2368	0.2256
	MAE	0.1938	0.3795	0.1866	0.1771
	Error _{pos}	0.1834	0.4052	0.1905	0.1746
	Error _{neg}	0.2055	0.0972	0.1808	0.179
NNGC1_dataset_D1_V1.010 (585, 5)	RMSE	0.0908	0.3931	0.0939	0.0849
	MAE	0.071	0.3781	0.0737	0.0692
	Error _{pos}	0.073	0.3781	0.0607	0.0724
	Error _{neg}	0.069	-	0.0827	0.0625

Table 12: (Continued) RMSE, MAE, Error_{pos}, and Error_{neg} values on the time series datasets for the proposed HE-LSSVR model against baseline models.

Dataset (No. of samples, No. of features)	Metric	SVR[4]	LS-SVR[17]	BLSSVR[43]	HE-LSSVR [†]
NNGC1.dataset.E1.V1.008 (740, 5)	RMSE	0.2226	0.4569	0.2182	0.2122
	MAE	0.1842	0.4083	0.1773	0.1711
	Error _{pos}	0.1644	0.4374	0.147	0.1251
	Error _{neg}	0.2103	0.1065	0.2194	0.2512
NNGC1.dataset.E1.V1.009 (740, 5)	RMSE	0.2132	0.4538	0.207	0.1995
	MAE	0.1778	0.4076	0.1641	0.1677
	Error _{pos}	0.1563	0.4267	0.1171	0.1325
	Error _{neg}	0.2068	0.1131	0.2293	0.2347
NNGC1.dataset.E1.V1.010 (650, 5)	RMSE	0.2676	0.4607	0.2662	0.2315
	MAE	0.2139	0.4073	0.2167	0.1661
	Error _{pos}	0.1866	0.4399	0.2139	0.1329
	Error _{neg}	0.2457	0.137	0.2238	0.2003
Average RMSE		0.243	0.4749	0.229	0.207

[†] represents the proposed model.

The boldface denotes the RMSE of the best model corresponding to each dataset.

Acknowledgment

This project is supported by the Indian government’s Science and Engineering Research Board (MTR/2021/000787) under the Mathematical Research Impact-Centric Support (MATRICS) scheme. The Council of Scientific and Industrial Research (CSIR), New Delhi, provided a fellowship for Mushir Akhtar’s research under grant no. 09/1022(13849)/2022-EMR-I.

References

- [1] S Larry Goldenberg, Guy Nir, and Septimiu E Salcudean. A new era: artificial intelligence and machine learning in prostate cancer. *Nature Reviews Urology*, 16(7):391–403, 2019.
- [2] Trevor Hastie, Robert Tibshirani, Jerome Friedman, Trevor Hastie, Robert Tibshirani, and Jerome Friedman. Overview of supervised learning. *The elements of statistical learning: Data mining, inference, and prediction*, pages 9–41, 2009.

- [3] Juan S Angarita-Zapata, Antonio D Masegosa, and Isaac Triguero. A taxonomy of traffic forecasting regression problems from a supervised learning perspective. *IEEE Access*, 7:68185–68205, 2019.
- [4] Harris Drucker, Christopher J Burges, Linda Kaufman, Alex Smola, and Vladimir Vapnik. Support vector regression machines. *Advances in Neural Information Processing Systems*, 9, 1996.
- [5] Corinna Cortes and Vladimir Vapnik. Support-vector networks. *Machine Learning*, 20(3):273–297, 1995.
- [6] Jing Dong, Liu Yang, Chang Liu, Wei Cheng, and Wenwu Wang. Support vector machine embedding discriminative dictionary pair learning for pattern classification. *Neural Networks*, 155:498–511, 2022.
- [7] Honorius Gâlmeanu and Răzvan Andonie. Weighted incremental–decremental support vector machines for concept drift with shifting window. *Neural Networks*, 152:528–541, 2022.
- [8] Robust cost-sensitive kernel method with Blinex loss and its applications in credit risk evaluation. *Neural Networks*, 143:327–344, 2021. ISSN 0893-6080. doi: <https://doi.org/10.1016/j.neunet.2021.06.016>.
- [9] Guo-Feng Fan, Meng Yu, Song-Qiao Dong, Yi-Hsuan Yeh, and Wei-Chiang Hong. Forecasting short-term electricity load using hybrid support vector regression with grey catastrophe and random forest modeling. *Utilities Policy*, 73:101294, 2021.
- [10] Quan Quan, Zou Hao, Huang Xifeng, and Lei Jingchun. Research on water temperature prediction based on improved support vector regression. *Neural Computing and Applications*, pages 1–10, 2022.
- [11] Ranjan Kumar Dash, Tu N Nguyen, Korhan Cengiz, and Aditi Sharma. Fine-tuned support vector regression model for stock predictions. *Neural Computing and Applications*, 35(32):23295–23309, 2023.
- [12] Junwei Ma, Ding Xia, Haixiang Guo, Yankun Wang, Xiaoxu Niu, Zhiyang Liu, and Sheng Jiang. Metaheuristic-based support vector regression for landslide displacement prediction: A comparative study. *Landslides*, 19(10):2489–2511, 2022.

- [13] Qiaochu Wang, Dongxia Chen, Meijun Li, Sha Li, Fuwei Wang, Zijie Yang, Wanrong Zhang, Shumin Chen, and Dongsheng Yao. A novel method for petroleum and natural gas resource potential evaluation and prediction by support vector machines (svm). *Applied Energy*, 351: 121836, 2023.
- [14] Qianglong Li, Dezhi Li, Kun Zhao, Licheng Wang, and Kai Wang. State of health estimation of lithium-ion battery based on improved ant lion optimization and support vector regression. *Journal of Energy Storage*, 50:104215, 2022.
- [15] Andrey Zahariev, Petko Angelov, and Silvia Zarkova. Estimation of bank profitability using vector error correction model and support vector regression. *Economic Alternatives*, 28(2):157–170, 2022.
- [16] Jongho Shin, H Jin Kim, and Youdan Kim. Adaptive support vector regression for UAV flight control. *Neural Networks*, 24(1):109–120, 2011.
- [17] Johan AK Suykens and Joos Vandewalle. Least squares support vector machine classifiers. *Neural Processing Letters*, 9:293–300, 1999.
- [18] K-R Müller, Alexander J Smola, Gunnar Rätsch, Bernhard Schölkopf, Jens Kohlmorgen, and Vladimir Vapnik. Predicting time series with support vector machines. In *International Conference on Artificial Neural Networks*, pages 999–1004. Springer, 1997.
- [19] Douglas M Hawkins. *Identification of outliers*, volume 11. Springer, 1980.
- [20] Ingo Steinwart and Andreas Christmann. *Support vector machines*. Springer Science & Business Media, 2008.
- [21] Ronan Collobert, Fabian Sinz, Jason Weston, and Léon Bottou. Trading convexity for scalability. In *Proceedings of the 23rd International Conference on Machine Learning*, pages 201–208, 2006.
- [22] Kuaini Wang and Ping Zhong. Robust non-convex least squares loss function for regression with outliers. *Knowledge-Based Systems*, 71:290–302, 2014.

- [23] Dalian Liu, Yong Shi, and Yingjie Tian. Ramp loss nonparallel support vector machine for pattern classification. *Knowledge-Based Systems*, 85: 224–233, 2015.
- [24] Liming Yang and Hongwei Dong. Robust support vector machine with generalized quantile loss for classification and regression. *Applied Soft Computing*, 81:105483, 2019.
- [25] Yafen Ye, Junbin Gao, Yuanhai Shao, Chunna Li, Yan Jin, and Xiangyu Hua. Robust support vector regression with generic quadratic nonconvex ε -insensitive loss. *Applied Mathematical Modelling*, 82:235–251, 2020.
- [26] Xijun Liang, Zhipeng Zhang, Yunquan Song, and Ling Jian. Kernel-based online regression with canal loss. *European Journal of Operational Research*, 297(1):268–279, 2022.
- [27] Jonathan T Barron. A general and adaptive robust loss function. In *Proceedings of the IEEE/CVF Conference on Computer Vision and Pattern Recognition*, pages 4331–4339, 2019.
- [28] Charlie Frogner, Chiyuan Zhang, Hossein Mobahi, Mauricio Araya, and Tomaso A Poggio. Learning with a wasserstein loss. *Advances in Neural Information Processing Systems*, 28, 2015.
- [29] Xu Li, Wei Chen, Chingyao Chan, Bin Li, and Xianghui Song. Multi-sensor fusion methodology for enhanced land vehicle positioning. *Information Fusion*, 46:51–62, 2019.
- [30] Xijiong Xie and Shiliang Sun. General multi-view semi-supervised least squares support vector machines with multi-manifold regularization. *Information Fusion*, 62:63–72, 2020.
- [31] Ping Zhong. Training robust support vector regression with smooth non-convex loss function. *Optimization Methods and Software*, 27(6): 1039–1058, 2012.
- [32] Subhash C Narula and John F Wellington. The minimum sum of absolute errors regression: A state of the art survey. *International Statistical Review/Revue Internationale de Statistique*, pages 317–326, 1982.

- [33] Pritam Anand, Reshma Rastogi, and Suresh Chandra. A new asymmetric ε -insensitive pinball loss function based support vector quantile regression model. *Applied Soft Computing*, 94:106473, 2020.
- [34] S Balasundaram and Yogendra Meena. Robust support vector regression in primal with asymmetric huber loss. *Neural Processing Letters*, 49:1399–1431, 2019.
- [35] Umesh Gupta and Deepak Gupta. On regularization based twin support vector regression with huber loss. *Neural Processing Letters*, 53(1):459–515, 2021.
- [36] Long Tang, Yingjie Tian, Chunyan Yang, and Panos M Pardalos. Ramp-loss nonparallel support vector regression: robust, sparse and scalable approximation. *Knowledge-Based Systems*, 147:55–67, 2018.
- [37] Dalian Liu, Yong Shi, Yingjie Tian, and Xiankai Huang. Ramp loss least squares support vector machine. *Journal of Computational Science*, 14:61–68, 2016.
- [38] Francesco Dinuzzo and Bernhard Schölkopf. The representer theorem for hilbert spaces: a necessary and sufficient condition. *Advances in Neural Information Processing Systems*, 25, 2012.
- [39] Léon Bottou, Frank E Curtis, and Jorge Nocedal. Optimization methods for large-scale machine learning. *SIAM Review*, 60(2):223–311, 2018.
- [40] Diederik P Kingma and Jimmy Ba. Adam: A method for stochastic optimization. *arXiv preprint arXiv:1412.6980*, 2014.
- [41] John Duchi, Elad Hazan, and Yoram Singer. Adaptive subgradient methods for online learning and stochastic optimization. *Journal of Machine Learning Research*, 12(7), 2011.
- [42] Tijmen Tieleman and Geoffrey Hinton. Lecture 6.5-RMSprop: Divide the gradient by a running average of its recent magnitude. *COURSERA: Neural Networks for Machine Learning*, 4(2):26–31, 2012.
- [43] Saiji Fu, Yingjie Tian, and Long Tang. Robust regression under the general framework of bounded loss functions. *European Journal of Operational Research*, 310(3):1325–1339, 2023.

- [44] Chih-Chung Chang and Chih-Jen Lin. Libsvm: a library for support vector machines. *ACM Transactions on Intelligent Systems and Technology (TIST)*, 2(3):1–27, 2011.
- [45] John Shawe-Taylor and Nello Cristianini. *Kernel methods for pattern analysis*. Cambridge University Press, 2004.
- [46] Dheeru Dua and Casey Graff. UCI machine learning repository. 2017.
- [47] Milton Friedman. A comparison of alternative tests of significance for the problem of m rankings. *The Annals of Mathematical Statistics*, 11(1):86–92, 1940.
- [48] Ronald L Iman and James M Davenport. Approximations of the critical region of the fbietkan statistic. *Communications in Statistics-Theory and Methods*, 9(6):571–595, 1980.
- [49] Janez Demšar. Statistical comparisons of classifiers over multiple data sets. *The Journal of Machine Learning Research*, 7:1–30, 2006.
- [50] J Derrac, S Garcia, L Sanchez, and F Herrera. KEEL data-mining software tool: Data set repository, integration of algorithms and experimental analysis framework. *J. Mult. Valued Logic Soft Comput*, 17, 2015.